Volume 27
Number 9
7 March 2025
Pages 2377-2596

# Green Chemistry

Cutting-edge research for a greener sustainable future

rsc.li/greenchem

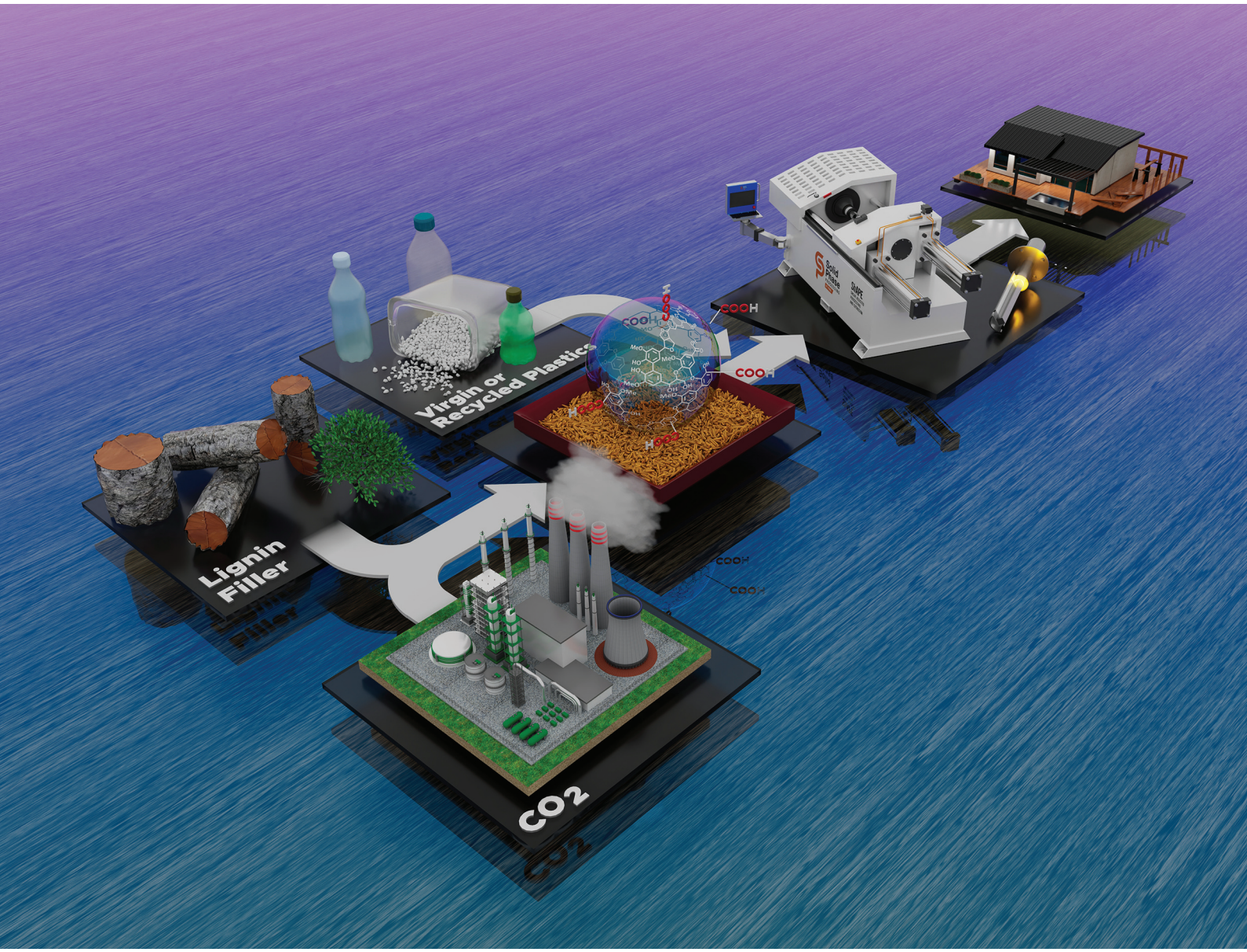


ISSN 1463-9262

ROYAL SOCIETY OF CHEMISTRY

**PAPER**
Satish K. Nune, David J. Heldebrant *et al.*
Carbon dioxide-negative composite materials: an economically viable solution for $CO_2$ sequestration

25 YEARS ANNIVERSARY

Green Chemistry

PAPER

View Article Online
View Journal | View Issue



Cite this: *Green Chem.*, 2025, **27**, 2392

# Carbon dioxide-negative composite materials: an economically viable solution for $CO_2$ sequestration†

Keerti S. Kappagantula,[a] Yuan Jiang,[a] Francesca Pierobon,[a,b] MD Reza E. Rabby,[a] Jose Ramos,[a] Yelin Ni,[a] Aditya Nittala,[a] Jaelynne King,[a] Ethan Nickerson,[a] Nicholas C. Nelson,[a] Wontae Joo,[a] Raveen John,[a] John C. Linehan,[a] Raul N. Aranzazu,[a] Satish K. Nune *[a] and David J. Heldebrant *[a,c]

Anthropogenic emissions of $CO_2$ have nearly exhausted our carbon budget, putting the world on a trajectory toward irreversible climate change. $CO_2$ emissions must be reversed in coming decades to avoid global warming past the 2 °C target. Recent approaches have focused on recycling $CO_2$ into fuels and chemicals to create sufficient financial incentives to pay for $CO_2$ removal and geological sequestration. These technologies aim to produce fuels and chemicals at quantities relevant to global markets while also recycling a meaningful amount of $CO_2$. While promising, these technologies are $CO_2$-neutral at best. Truly negative emission technologies will require significant quantities of durable, fungible products that sequester hundreds of millions of tonnes of $CO_2$. We present an economically viable approach to sequestering hundreds of thousands of tonnes of $CO_2$ per year in polymer composites made from $CO_2$-functionalized lignin or lignite fillers mixed with a high-density polyethylene (HDPE) matrix. $CO_2$ is chemically fixed to polymeric phenols *via* C–C bond formation at the lignin or lignite surface, storing about 2–4.2 wt% of $CO_2$. Composites produced with the $CO_2$-functionalized fillers and HDPE have mechanical properties that meet international building code standards for decking, a multi-billion-dollar market. A techno-economic analysis and life cycle assessment suggest that $CO_2$-functionalized lignin and lignite fillers have favorable economic potential. These composites could reduce greenhouse gas emissions up to 62% over conventional wood plastic composites or be $CO_2$-negative within 20 years when manufactured with renewable electricity, recycled high-density polyethylene and if extra $CO_2$ is captured and sequestered in the ground. The composites can achieve a net-negative global warming potential after 54 years for the $CO_2$ solely stored in the composites.

Received 7th November 2024,
Accepted 14th January 2025

DOI: 10.1039/d4gc05692b

rsc.li/greenchem



## Green foundation

1. We combined three industrial wastes, $CO_2$, lignin, and high-density polyethylene plastic and reconstitute them into a $CO_2$-negative building composite that meets international building codes. These composites reduce greenhouse gas emissions by avoiding the combustion of waste lignin while also chemically storing exogenous $CO_2$ on the lignin embedded in a plastic matrix.
2. We have developed a novel green process that produces fungible composite materials from large-volume wastes with significantly lower environmental impact than wood plastic composites and associated manufacturing processes.
3. The work could be made greener by expanding the types of recycled plastics, the amount of lignin combustion avoided, and $CO_2$-sequestration potential. This can be achieved by (a) adapting $CO_2$ fixation to other large-volume bio or aromatic polymers, (b) expanding matrix selection to other plastics such as nylon and polyester, and (c) producing other products for fencing, siding and structural applications.

[a]*Pacific Northwest National Laboratory, Richland, WA 99354, USA. E-mail: satish.nune@pnnl.gov, david.heldebrant@pnnl.gov*
[b]*School of Environmental and Forest Sciences, University of Washington, Seattle, Washington 98195, USA*
[c]*Department of Chemical Engineering, Washington State University, Pullman, WA 99163, USA*

† Electronic supplementary information (ESI) available. See DOI: https://doi.org/10.1039/d4gc05692b

## Introduction

The combustion of fossil fuels releases heat-trapping gasses, including carbon dioxide ($CO_2$), that drive the greenhouse effect behind anthropogenic climate change.[1,2] To mitigate these effects, it is widely accepted that the global economy will need to transition to net-zero emissions which will require $CO_2$ removal from hard to decarbonize sectors.[3–6] $CO_2$ capture from concentrated point-sources ranges from $47–80 (USD) per tonne $CO_2$ [7] and does not directly reduce the amount of carbon dissolved in the air and ocean. Reducing the impact of greenhouse gases requires the removal of legacy emissions through negative-emission technologies (NETs). NETs, such as direct air capture, are effective but expensive at $150–1000 (USD) per tonne $CO_2$.[8,9] Geological sequestration adds another $20 per tonne $CO_2$,[10] making NETs cost-prohibitive without regulatory requirements or economic incentives.

We previously made the case that an alternative NET approach was to provide economic incentives for purchasing "green" $CO_2$-derived products that could be complimentary to tax credits such as 45Q.[11–13] Many materials and chemicals could be made from $CO_2$;[14] however, these markets remain small outside of enhanced oil recovery and niche uses of $CO_2$ for agriculture. The recent surge in efforts to upcycle $CO_2$ into commodity chemicals or fuels has produced approaches that are $CO_2$-neutral at best.[15–17] There is renewed interest in $CO_2$-negative technologies,[18,19] including cement-based products[20,21] and other building materials.[21,22] This interest has led to a pressing need to create new markets and a broader mix of value-added materials made from $CO_2$ to expand sequestration potential and market penetration.

Establishing new materials at scales relevant to annual $CO_2$ emissions requires sourcing reagents at comparable scales and costs to $CO_2$. Building materials such as decking,[23] made with "engineered" composites also called wood plastic composites (WPC),[24–26] represent a multibillion dollar per year market producing 3.55 billion linear board feet or approximately ~3.55 billion kg of material. They are made by mixing and extruding HDPE with about 50–60 wt% wood flour, typically obtained as sawmill waste.[23–25] Recent research has focused on replacing the wood flour with large volume complex biopolymer fillers like lignin or lignite given their abundance, low cost, chemical stability, lower susceptibility to rot, higher flash points, and UV tolerance, which could improve material performance without increasing costs.[26] Lignin is renewable organic cross-linked polyphenol polymer byproduct from the pulp and paper industry that is burned to power the pulping process, produced at roughly 50 MMt per yr.[28] Lignite (the lowest rank of coal) is a cross-linked polyphenol polymer that is effectively waste because it is more costly to ship than to burn. Replacing wood flour with lignin or lignite as fillers in building materials, such as decking, presents an opportunity to use these materials. Their use avoids greenhouse gas emissions from burning or accumulation in landfills, with the added potential for conversion of waste into "green" fillers that sequester exogeneous $CO_2$ on their surfaces.

The polyphenolic composition of lignin and lignite allows for chemical fixation of $CO_2$ by means of the ubiquitous Kolbe–Schmitt (KS) reaction.[27–29] KS reactions proceed (Fig. 1a) by deprotonation of an aromatic alcohol by a Brønsted base, resulting in a breaking of aromaticity and forming the corresponding enol, which then acts as a nucleophile to attack the central carbon of $CO_2$, followed by deprotonation of the aromatic H to then re-establish aromaticity. The reaction is completed after acid-washing, resulting in a carboxylic acid most commonly at the *ortho* or *para* positions to the phenol moiety. Chemically fixation of $CO_2$ as carboxylic acids is preferrable because the $CO_2$ is chemically bound to the aromatic ring by carbon–carbon bonds, lessening the chance of $CO_2$ release by common degradation pathways such as hydrolysis.[30] There have been reports of carboxylation reactions of monomers of lignin and lignite[31] as well as the carboxylation of lignin particles, suggesting that any polymer with sufficient phenol content could be a candidate $CO_2$-negative filler.[31,32]

The pathway for replacing wood flour with lignin and lignite $CO_2$-functionalized fillers is attractive, but only viable if the mechanical properties of the final composites are on par with or better than conventional WPCs. Emerging evidence shows that the mechanical properties of composites made from lignin and lignite fillers are lower than those of WPCs.[26] But it is well known that increasing the concentration of fillers (the load bearing component) can result in composites with higher mechanical properties. Additionally, lignin and lignite fillers with surface functionalities may have better interaction with the HDPE matrix. However, it is challenging to introduce >60 wt% fillers through traditional composite manufacturing routes given their inability to accommodate the higher viscosity of the feedstock. Manufacturing approaches that can accommodate high filler loadings such as compression molding may not be suitable for the high-volume production required for building material applications. Shear based processes such as friction extrusion may be suitable for manufacturing such composites as they can accommodate the high filler loading while facilitating intimate mixing between the constituent components, essential for achieving final products with uniform properties.

We present an experimental and modeling study that assesses a new class of $CO_2$-negative composites comprised of lignin or lignite fillers functionalized with carboxylic acids (captured $CO_2$) mixed in a HDPE matrix. We detail the rates and yield of carboxylation of varied lignin and lignite precursors. We describe the characterization and quantification of the $CO_2$ content of carboxylated lignin and lignite particles. Composite manufacturing was performed using conventional injection molding with 50 wt% filler and friction extrusion using the shear-assisted processing and extrusion process (ShAPE) platform with 80 wt% filler.[33] We tested the composites for mechanical properties to qualify them as potential building materials per IBC metrics. We present a preliminary techno-economic (TEA) and life cycle assessment (LCA) of a process where composites are produced with lignite or lignin,

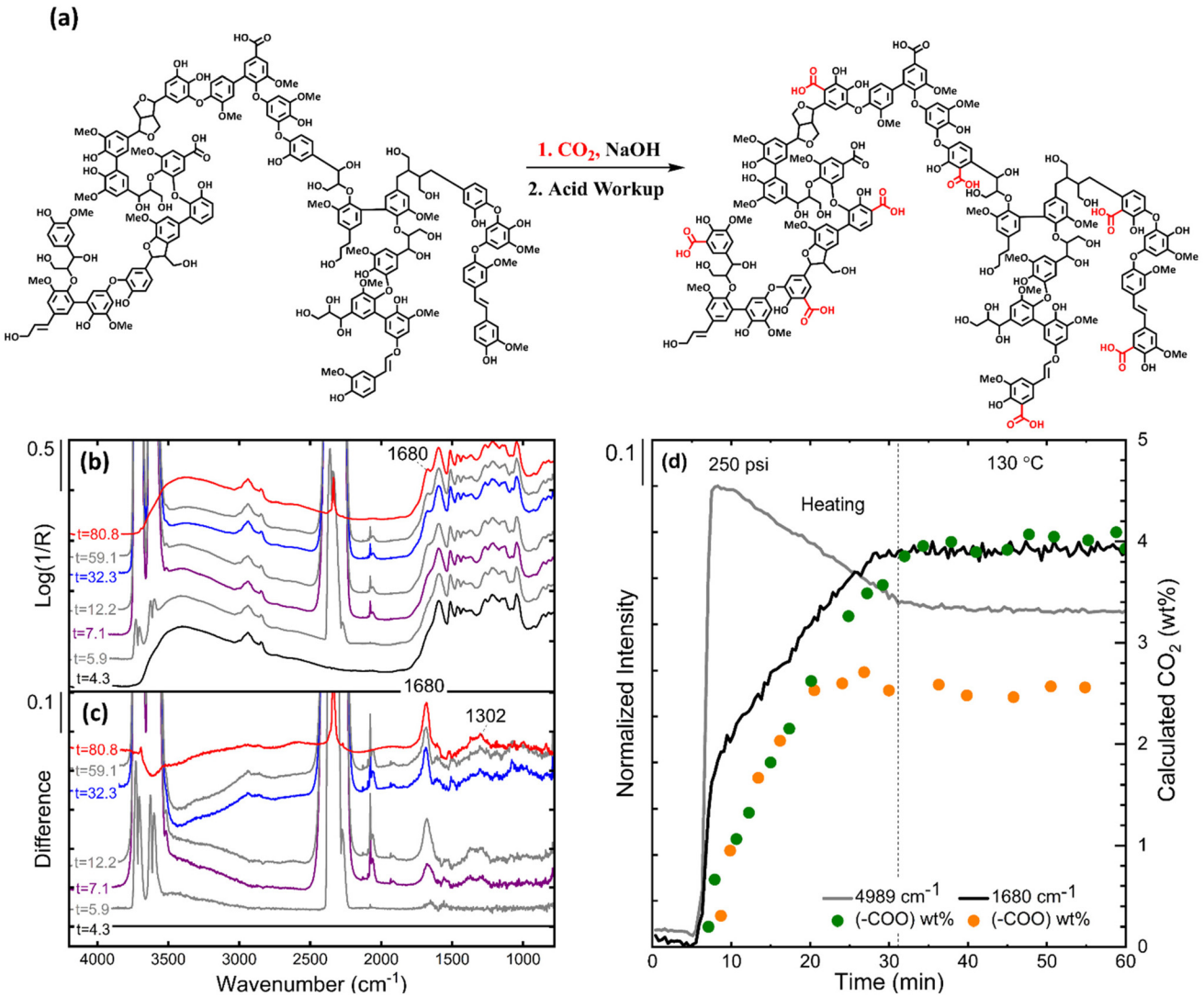


**Fig. 1** (a) Schematic representation of the Kolbe–Schmitt reaction of alkaline lignin showing the addition of $CO_2$ in the form of a carboxylic acid highlighted in red. (b) Stacked log(1/*R*) FTIR spectra of alkaline lignin during various time points of the Kolbe–Schmitt process using a high temperature DRIFTS cell starting with the alkaline lignin spectrum shown at timepoint 4.3 min. Introduction of $CO_2$, indicated by the combination bands above 3500 $cm^{-1}$ and the oversaturation of the stretching band in the grey spectrum taken at timepoint 5.9 min. At 7.1 min, shown in the purple spectrum, a final pressure of 250 psi was reached in the DRIFTS cell. The formation of a shoulder at 1680 $cm^{-1}$ shown in the spectrum taken at time point 12.2 min indicates the formation of the product peak. At 32.3 min, shown in blue, has a distinct peak growing at 1680 $cm^{-1}$ as the final temperature of 130 °C was reached. An isothermal hold for 30 minutes, indicated by the spectrum taken timepoint 59.1 min shown in grey, shows a distinct peak at 1680 $cm^{-1}$. Lastly, the final spectrum of the sample at room temperature and under nitrogen purge taken at timepoint 80.8 min shows a new peak at 1680 $cm^{-1}$, the only significant change to the alkaline lignin spectrum. (c) The difference spectra are a result of the alkaline lignin spectrum taken at time point 4.3 min (black) subtracted from the remaining spectra to highlight the key changes to the sample. The difference spectra show the evolution of the anionic carboxylate peak at 1680 $cm^{-1}$ as the reaction progresses. Additional peaks are observed at 1302 $cm^{-1}$ indicating *ν*(C–O). (d) Intensity profiles over the duration of the *in situ* Kolbe–Schmitt experiment of $CO_2$ (4989 $cm^{-1}$) and the anionic carboxylate $COO^-$ (1680 $cm^{-1}$) peak. The profiles highlight various stages of the reaction. The profile of 4989 $cm^{-1}$ representing $CO_2$ increases as the cell is pressurized to 250 psi then decreases at the cell was heated to 130 °C before plateauing during the isothermal hold. The profile of 1680 $cm^{-1}$ representing the product increases as the cell is pressurized indicating uptake, then gradually increases as the cell reaches 130 °C before plateauing during the isothermal hold. Scattered plots of the quantified amount of $CO_2$ (wt%) added to the lignin during the experiment is shown for an alkaline lignin sample (●) and an anhydrous alkaline lignin-sodium hydroxide sample (●).

recycled HDPE, and renewable energy to reduce greenhouse gas emissions and sequester tens to hundreds of thousands of tonnes of $CO_2$ per year. The products would achieve a predicted negative global warming potential over an assumed product lifetime. The envisioned process shows favorable economics and could turn a profit, a rarity for a negative emission approach. We conclude with a discussion on the processing and manufacturing challenges needed for commercialization as well as $CO_2$ sequestration potential in other composite markets.

 

## Results and discussion

### Carboxylation of lignin or lignite biopolymers

Carboxylation of lignin or lignite biopolymers was achieved by reacting as received lignin or lignite (ground and sieved with a 625 mesh) with NaOH under elevated pressure and temperature (Table 1).[34] Specific details and characterization of the carboxylation can be found in the ESI.† In a typical reaction, the carboxylation of lignin or lignite was achieved by mixing a base with 1–500 g of raw particles in a sealed stainless-steel autoclave under air. After the phenol deprotonation was complete, water was removed by venting. The reactor was then charged with a known volume of $CO_2$ and sealed. The reactor was heated to a desired temperature and the pressure logged. The final pressure was logged to track $CO_2$ consumption before the reactor was cooled to room temperature and vented. The carboxylated particles were isolated after being worked up with an aqueous solution of acid, filtered through a medium porosity fritted glass filter, and dried in a vacuum oven.

Confirmation of $CO_2$ capture was achieved by reacting $^{13}C$-enriched $CO_2$ at 120 °C with lignin in custom high-pressure WHiMS magic angle spinning nuclear magnetic resonance (NMR) rotors.[35–37] *In situ* NMR showed the presence of a $^{13}C$-enriched carboxylate at ~160 ppm (Fig. S1†). The peak remained after *in situ* acid workup with dilute $H_2SO_4$ (Fig. S2†), confirming the moiety's identity as a carboxylic acid.

As $^{13}C$ NMR is not truly quantitative, the carboxylic acid content on lignin or lignite was quantified using Fourier transform infrared (FTIR) spectroscopy.[38] The results are provided below in Table 1. Carboxylate content was calculated based on the log(1/*R*) spectrum of the carbonyl peak centered around 1685 $cm^{-1}$. Fig. 1(b and c) shows the log(1/*R*) spectra for alkaline lignin before, during, and after the *in situ* carboxylation reaction. Carboxylation yields for alkaline lignin varied between 2.5–4 wt%, depending on equivalents of base, reaction temperature, and pressure. Carboxylation yields for lignite plateaued at 2.0 wt% regardless of additional base. Higher carboxylation yields for lignin over lignite were expected due to lignin's higher concentration of phenol groups (Table 1). Unsurprisingly, alkaline lignin showed the highest uptake, which we attribute to the Brønsted basic nature of sodium phenolate and sodium carboxylate moieties on the particle's surface.

Alkaline lignin naturally contains 1–2 wt% sodium carboxylate moieties that become carboxylic acids during workup. These naturally occurring acid groups on alkaline lignin also have a carbonyl stretching vibration for the carboxylic acid at 1714 $cm^{-1}$, complicating the differentiation of the newly added carboxylic acids from the naturally occurring carboxylate groups. As other sources of lignin do not contain meaningful amounts these carboxylates, we posit that sufficiently basic alkaline lignin could slowly undergo natural carboxylation by absorbing from $CO_2$ in the air. We are not considering these natural acids in our analysis.

We used *in situ* DRIFTS (diffuse reflectance infrared Fourier transform spectroscopy) to track the carboxylation reaction (Fig. 1a). The DRIFTS measurements were calibrated using a sample mixture of the substrate (alkaline lignin, lignite) with varying amounts of benzoic acid. The calibration standards produced an IR spectrum analogous to the *in situ* spectrum of the product shown in Fig. S3.† Fig. 1b shows DRIFTS results of the *in situ* reaction performed with alkaline lignin in the absence of NaOH. Baseline carboxylation was first attempted on the raw alkaline lignin particles given their inherent basicity (pH 9–10). The log(1/*R*) spectrum in Fig. 1b shows the presence of a shoulder peak representative of a carboxylic salt carbonyl group at 1685 $cm^{-1}$. The $CO_2$ contains two unique carbon–oxygen bonds due to resonance structures that produce two peaks in the infrared spectrum. It is important to note the absence of the corresponding symmetric vibration at a lower wavenumber. The 1685 $cm^{-1}$ band is more prominent in the IR difference spectra of alkaline lignin (Fig. 1c) before and after the reaction, calculated by subtracting the log(1/*R*) spectrum of alkaline lignin before reaction (under $N_2$ gas) taken at time point 4.3 min, from the log(1/*R*) spectrum of the alkaline lignin under a $CO_2$ purge (5.9 min, grey), 250 psi of $CO_2$ (7.1 min, purple), 130 °C (32.3 min, blue), and nitrogen purge (depressurization)(80.8 min, red). Fig. 1d shows the intensity *versus* time of $CO_2$ and the carbonyl peak of carboxylate at 1680 $cm^{-1}$ as well as the calculated wt% $CO_2$ added to alkaline lignin with and without sodium hydroxide as a scatter plot. The carbonyl content (wt%) was calculated from the area of the band at 1680 $cm^{-1}$ from the log(1/*R*) spectrum. The addition of sodium hydroxide increases the pH of the lignin from 8–10 to 14. The increase in basicity results in the deprotonation of additional hydroxyl groups, leading to increased uptake of $CO_2$ from 2.5 wt% to 4.0 wt% (Fig. 1c). It should be noted that the 1680 $cm^{-1}$ band intensity decreases once the cell is purged with nitrogen at room temperature without the final acid work up of the product. A follow up publication will detail the effect of acid washing.

**Table 1** Summary of carboxylation yields of alkaline lignin and lignite quantified after *in situ* Kolbe–Schmitt* experiments. The $CO_2$ wt% is quantified based on area analysis of the IR spectra after the cell was vented

| Material | $CO_2$ (wt%) | Lignin (g) : NaOH (mmol) |
|---|---|---|
| Alkaline lignin | 2.5 | 1 : 0 |
| Alkaline lignin | 4.0 | 1 : 1 |
| Lignite | 0 | 1 : 1 |
| Lignite | 2.0 | 1 : 2 |
| Lignite | 2.0 | 1 : 3 |

*Experiments run at 130 °C and 250 psi $CO_2$.

### Composite manufacturing and testing

Virgin HDPE (Microthene® FA 700–00, LyondellBasell) was chosen as the matrix for the composites. We used virgin HDPE in this study to enable direct comparison to WPCs in the literature. Eventually, recycled HDPE or low-density polyethylene

(LDPE) will be used to provide a lower greenhouse gas footprint. Composites were manufactured into flexural samples of 3 mm thick × 12.7 mm wide × 58.4 mm long per American Society for Testing and Materials (ASTM) D790 and tested, as shown in Fig. 2. Composite constituents were dry-mixed in predetermined material ratios using a ball mill, then melt-compounded and granulated (Fig. 2a). Polymer composites were then either injection molded (Fig. 2b) or friction-extruded *via* the ShAPE™ platform (Fig. 2c).[33] The injection molded samples were directly manufactured as ASTM D790 specimens, while the friction extruded samples were manufactured as bars with a 3 mm × 12.7 mm rectangular profile *via* the ShAPE machine and then machined into 58.4 mm long specimens. Baseline composites were made with unfunctionalized filler and $CO_2$-negative composites were made using $CO_2$-functionalized lignin and lignite fillers. Lignin polymer composites made by injection molding were limited to 50 wt% filler due to high viscosity, lack of mixability, and the presence of voids at higher loadings. Conversely, composites made on the ShAPE platform achieved 80 wt% filler concentrations as the high shearing forces and friction combine to plasticize and flow the material to form extrudate free of voids. WPC boards from commercial suppliers, specifically TimberTech Azek and Trex Transcend, were procured, machined into flexural samples, and tested alongside the composites to establish commercial performance baselines.

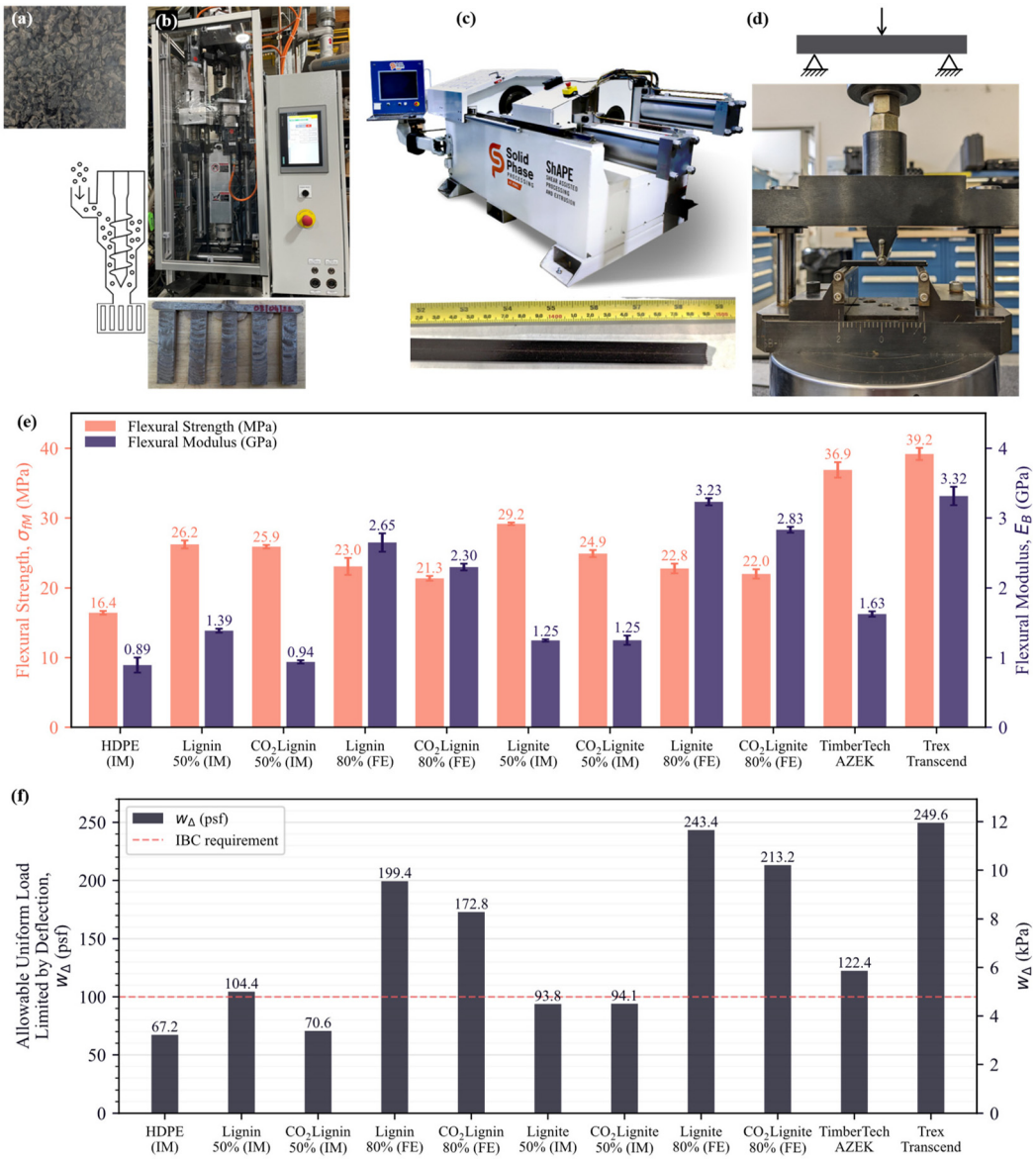


**Fig. 2** Lignin/lignite polymer composite manufacturing and flexural properties. (a) pelletized lignin or lignite melt compounded with HDPE, (b) injection molding and molded flexure specimens, (c) ShAPE machine and friction extruded composite bars, (d) flexure testing, (e) flexural strength and modulus of injection molded (IM) and friction extruded (FE) lignin and lignite polymer composites with 50 and 80 wt% $CO_2$-functionalized and unfunctionalized fillers, and (f) uniform live load allowable for the materials determined per IBC guidelines.

Friction extruded samples manufactured *via* the ShAPE platform exhibited high flexure performance as shown in Fig. 2e, allowing a high uniform live load that exceeded the standard decking materials on the market (Fig. 2f). Addition of 80 wt% carboxylated lignin and lignite led to an increased flexural modulus compared to the injection molded composites at 2.30 GPa and 2.83 GPa, respectively. Addition of 80 wt% unfunctionalized fillers resulted in a higher flexural modulus of 2.65 GPa (lignin) and 3.23 GPa (lignite). The improvement in flexural performance of the friction extruded 80 wt% filler composites is attributed to the higher filler content that increased overall stiffness of the material system. It may also be due to the higher forces used while manufacturing, which seem to have enhanced the consolidation between the HDPE matrix and the filler to facilitate better load transfer.

For comparison, injection molded lignin and lignite polymer composites with 50 wt% unfunctionalized fillers showed flexural moduli of 1.39 GPa (lignin) and 1.25 GPa (lignite) (Fig. 2d). Injection molded lignin polymer composites with 50 wt% carboxylated lignin showed a lower flexural modulus of 0.94 GPa. However, the flexural modulus of the 50 wt% $CO_2$-lignite composite was similar to that of a 50 wt% lignite composite at 1.25 GPa. Commercial decking materials showed a flexural modulus of 1.63–3.32 GPa in comparison. The friction extruded lignin and lignite composites with 80 wt% $CO_2$ functionalized filler showed a flexural modulus comparable to or higher than that of some commercial decking materials. Commercial decking boards are typically manufactured with both virgin and recycled HDPE as well as LDPE. They use manufacturing processes capable of introducing at most 50–60 wt% fillers, while our friction extruded composites contain 80 wt% fillers. We anticipate at least a 10–15% decrease in the mechanical properties when recycled polymers or LDPE are used as matrix materials in place of virgin polymers. These reductions can be offset with further recipe refinement, such as the addition of compatibilizers for stronger interfacial bonding.

While carboxylation did not affect the flexural modulus of injection molded lignite composites, it decreased the flexural strength in the 50 wt% $CO_2$-lignite composite which showed nearly 15% lower flexural strength than a 50 wt% lignite composite. Contrarily, carboxylation did not significantly affect the flexural strength of the injection molded, friction extruded, and 80 wt% lignite composites. Interestingly, the flexural strength of all composites manufactured in this study was lower than those of the commercial decking materials. This difference is likely due to the absence of compatibilizers that can enhance the interaction between filler and polymer matrix that are usually included in commercial decking materials.

For a polymer composite to be a usable decking material, the deflection in the polymer composite decking board caused by live load must be smaller than $l/360$, where $l$ is the span. Additionally, the minimum uniformly distributed live load must be 1.5 times the live load for the area served without exceeding 100 psf (4.79 kPa).[39] Fig. 2f shows the allowable uniform live load for polymer composites manufactured *via* injection molding and friction extrusion *via* ShAPE for a span ($l$) of 16 in (40.64 cm), a deflection ($l/360$) of 0.044 in (0.11 cm), and a board thickness of 0.94 in (2.39 cm). The span and thickness values were typical for a 1 in × 6 in (2.54 cm × 15.24 cm) commercial decking boards.

The injection molded composites with 50 wt% unfunctionalized lignin fillers can be used as decking materials per IBC metrics. However, it evident that injection molded composites with carboxylated fillers are not qualified for use as decking materials as their uniform live load bearing capacity is less than the IBC threshold of 100 psf (4.79 kPa). Increasing the filler content to 80 wt% *via* the ShAPE platform resulted in enhanced flexural modulus and correspondingly increased allowable uniform live loads. Friction extruded composites with 80 wt% unfunctionalized lignite showed the highest live load bearing capacity of 243.38 psf (11.65 kPa) for a projected span rating of 16 in (40.64 cm), giving decking boards made from the material sufficient room for increasing their span to 20 in (50.8 cm). While the functionalized lignin composites demonstrate a comparatively lower allowable uniform live load of 172.8 psf (8.27 kPa) for a span rating of 16 in (40.64 cm), they are qualified to be used as building materials well, as the value is higher than the required threshold of 100 psf (4.79 kPa) required by the IBC. Additional properties important for qualifying a composite as a building material will be the topic of follow-on studies. It is worth noting that the mechanical performance of the lignin composites with functionalized fillers, especially those with high filler content (≥80 wt%), may benefit from the use of compatibilizers.

### Techno-economic assessment

Experimental data were used to develop rigorous process models for the carboxylation unit in Aspen Plus to provide mass and energy balance data for a TEA and LCA. Key model inputs for the two lignin and one lignite cases investigated in this study are summarized in Fig. 3. For lignin, two acid workup and product recovery approaches were investigated—one using HCl and one using $H_2SO_4$. For lignite, only an $H_2SO_4$ based approach was studied. The modeling approach and key assumptions can be found in the methods section in the ESI† and the mass and energy balance are in Table S3.† Table 2(a) presents the modeled minimum selling price of the carboxylated lignin or lignite fillers. As shown in Table 2(a), both the lignin-HCl case and lignite-$H_2SO_4$ case can produce $CO_2$LIG filler at a cost comparable to the market price of HDPE ($1 per kg), confirming their economical use as filler. Lignin-$H_2SO_4$ has lower utility and chemical costs than lignin-HCl because the vacuum dryers needed for the lignin-HCl process consume significant amounts of energy and $H_2SO_4$ is much cheaper than HCl. However, the minimum $CO_2$LIG selling price of the lignin-$H_2SO_4$ is still higher than lignin-HCl case due to the lower $CO_2$LIG recovery rate (65% *vs.* 88%), higher capital costs, and higher wastewater treatment costs. The lignin-$H_2SO_4$ case is still under optimization, which lead to a reduced estimated production cost relative to the already optimized lignite system. A $CO_2$LIG recovery rate up to 88%

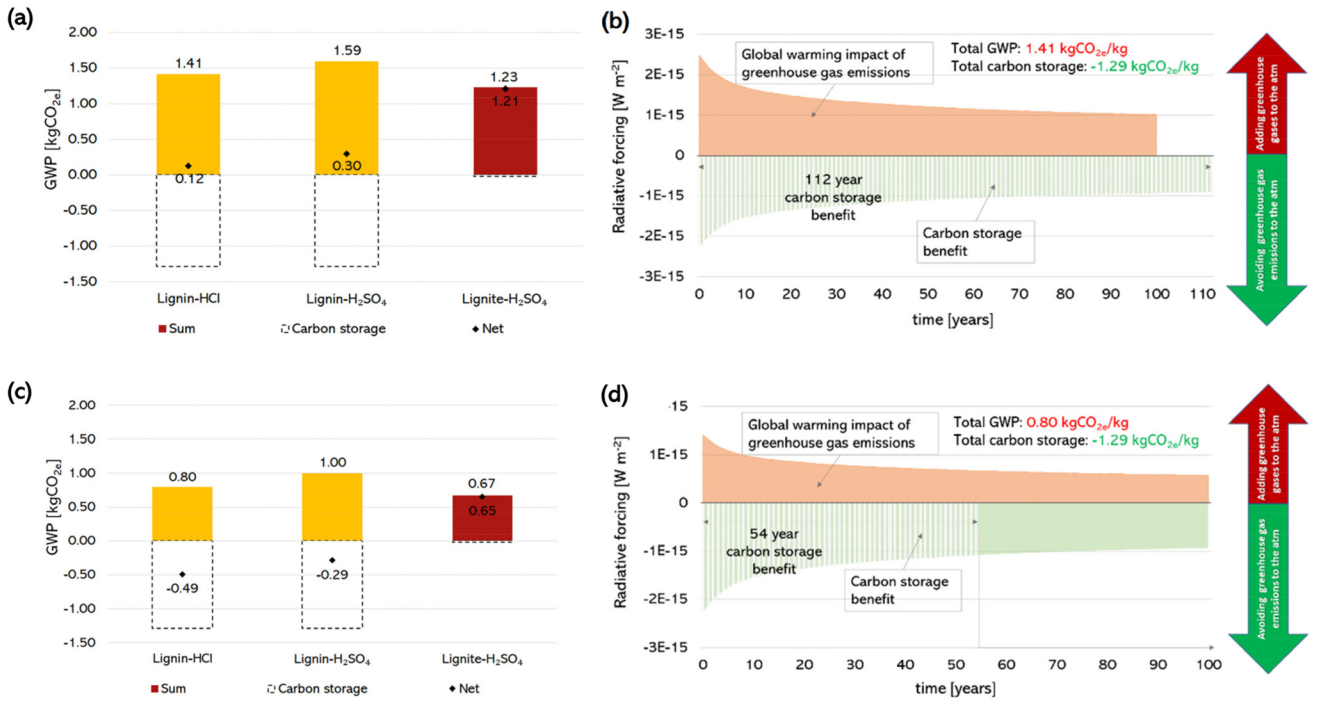


**Fig. 3** Life cycle assessment. (a) Global warming potential results for 1 kg of composite panel for the lignin-HCl, lignin-$H_2SO_4$, and lignite-$H_2SO_4$ base case scenarios, respectively. (b) Life cycle greenhouse gas emissions and carbon storage benefits using a temporal radiative forcing analysis for the base case scenario for lignin-HCl. (c) Global warming potential results for 1 kg of composite panel in alternative scenarios (100% recycled HDPE and renewable electricity) for the lignin-HCl, lignin-$H_2SO_4$, and lignite-$H_2SO_4$ cases, respectively. (d) Life cycle greenhouse gas emissions and carbon storage benefits using temporal radiative forcing analysis for the alternative scenario for lignin-HCl.

has been successfully demonstrated for lignite-$H_2SO_4$. Comparing the two $H_2SO_4$ cases, lignite has a much higher chemical cost than lignin as the carboxylation step consumes twice as much NaOH leading to increased $H_2SO_4$ consumption. However, lignite is much cheaper than lignin, so the feedstock cost is lower. The higher $CO_2$LIG recovery rate and shorter reaction time results in lower waste disposal and capital costs for the lignite case and much lower capital and fixed operating costs due to economies of scale. The minimum $CO_2$LIG filler selling price for the lignite case is \$0.37 per kg, comparable to the market price of wood flour and 71% lower than that of the lignin-$H_2SO_4$ case and 55% lower than the lignin-HCl case.

## Life cycle assessment

An LCA was performed on the envisioned process (the assumptions and details are provided in the methods section of the ESI†).[40,41] The results of the LCA for Global Warming Potential (GWP) are shown in Fig. 3. In the base case scenario (Fig. 3a), the total GWPs of 1 kg of $CO_2$LIG-plastic composite panel were 1.41, 1.59, and 1.23 kg carbon dioxide equivalents ($CO_{2e}$) for the lignin-HCl, lignin-$H_2SO_4$, and lignite-$H_2SO_4$ cases, respectively. The carbon storage benefit was −1.29 $kgCO_{2e}$ for the lignin case and −0.02 $kgCO_{2e}$ for the lignite case per kg of $CO_2$LIG-plastic composite panel over a 100-year time horizon. This benefit included both the carbon stored in the lignin and the sequestered $CO_2$ in the panel. Therefore, the net GWP results were 0.12, 0.30, and 1.21 $kgCO_{2e}$ for the lignin-HCl, lignin-$H_2SO_4$, and lignite-$H_2SO_4$ cases, respectively. Alternative scenarios (Fig. 3c) included: (i) replacing HDPE with recycled HDPE and (ii) replacing electricity from the grid with 100% renewable electricity. In all the alternative scenarios, GWP results were net negative for the lignin case when considering carbon storage benefits, with values ranging between −0.49 and −0.29 $kgCO_{2e}$ over a 100-year time horizon. The net GWP for lignite in the alternative scenario was 0.65 $kgCO_{2e}$.

Considering the U.S. average industrial recycling rate for HDPE of 29.3% (EPA, 2017),[42] the total GWPs of 1 kg of $CO_2$LIG-plastic composite panel were 1.07, 1.24, and 0.89 kg $CO_{2e}$ for the lignin-HCl, lignin-$H_2SO_4$, and lignite-$H_2SO_4$ cases, respectively. Including the carbon storage benefit, net GWP results were −0.22, −0.05, and 0.87 $kgCO_{2e}$ for the lignin-HCl, lignin-$H_2SO_4$, and lignite-$H_2SO_4$ cases, respectively. When considering the U.S. average industrial recycling rate for HDPE and 100% renewable energy, the total GWPs of 1 kg of $CO_2$LIG-plastic composite panel were 0.94, 1.14, and 0.82 kg $CO_{2e}$ for the lignin-HCl, lignin-$H_2SO_4$, and lignite-$H_2SO_4$ cases, respectively. Including the carbon storage benefit, net GWP results were −0.35, −0.15, and 0.79 $kgCO_{2e}$ for the lignin-HCl, lignin-$H_2SO_4$, and lignite-$H_2SO_4$ cases, respectively.

The GWP for the lignin-$H_2SO_4$ case was slightly higher than for lignin with HCl treatment; the percentage increase ranging between 13% and 25% depending on the scenario (Fig. 3a and c). The higher impact comes from the larger amount of acid

 

**Table 2** Techno-economic assessment. (a) Estimated minimum selling price of $CO_2$LIG filler. (b) Operating condition and performance measures of the carboxylation unit used in TEA and LCA studies

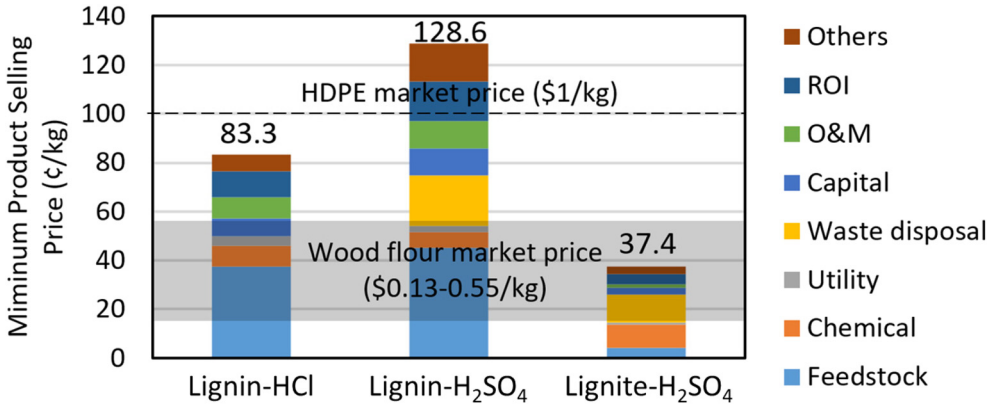


| | Lignin-HCl | Lignin-$H_2SO_4$ | Lignite-$H_2SO_4$ |
|---|---|---|---|
| NaOH treatment | | | |
| Solvent (per g lignin per lignite) | 1 ml 1 M NaOH | 1.5 ml 0.67 M NaOH | 2 ml 1 M NaOH |
| Temperature/pressure | Room | Room | Room |
| Residence time | 3 h | 3 h | 1 h |
| Water removal | Vacuum dryer @ 130 °C | Filtration | Filtration |
| Carboxylation | | | |
| Temperature/pressure | 130 °C, 15 bar | 130 °C, 15 bar | 130 °C, 28 bar |
| Residence time | 3 h | 3 h | 1 h |
| Acidification | | | |
| Acid (per g lignin per lignite) | 1 ml 2 M HCl | 3 ml 0.67 M $H_2SO_4$ | 2 ml 1 M $H_2SO_4$ |
| Temperature/pressure | Room | Room | Room |
| Residence time | 5 min | 5 min | 5 min |
| $CO_2$LIG Recovery | | | |
| Wash (per g lignin) | 200 ml acetone (5% $H_2O$) | 100 ml ice water | 100 ml 25 °C water |
| Separation | Vacuum dryer @ 130 °C | Filtration | Filtration |
| $CO_2$LIG recovery rate | 80% | 65% | 88% |
| Waste Stream Treatment | Acetone recycled; lignin sent to burner | Quick lime to adjust pH; then send to waste water treatment | Quick lime to adjust pH; then send to wastewater treatment |

needed in the acidification process and the lower yield of $CO_2$LIG production. The results for the lignite case were lower than the lignin case due to the lower impact of extracting lignite compared to separating lignin through the LignoBoost process. Compared to conventional wood-plastic composites, the GWPs of the $CO_2$LIG-plastic composite panel had lower impacts across all scenarios, with an overall GWP reduction between 9 and 62% (carbon storage benefits excluded).[43]

The results presented in Fig. 3a and c were based on a fixed 100-year time horizon for both the global warming impact of fossil-based greenhouse gas emissions and the carbon storage benefits. We also performed a temporal radiative forcing analysis to calculate the number of years of storage (*i.e.*, lifetime of the product) needed to achieve carbon neutrality.[44] The base case and alternative scenario for the lignin-HCl case are represented in Fig. 3b and d respectively. The red area on the positive side of the *y*-axis represents the cumulative radiative forcing associated with fossil-based greenhouse emissions released within the life cycle of 1 kg of $CO_2$LIG panel. The green area on the negative side of the *y*-axis represents the radiative forcing associated with the carbon storage benefits. Carbon neutrality is achieved when the red area equals the green area. In Fig. 3b, carbon neutrality is achieved after 112 years, *i.e.*, after the 100-year time horizon. In Fig. 3d, carbon neutrality is achieved after 54 years of carbon storage. This means that storing carbon for more than 54 years would result in a net negative GWP.[45–47]

It may be noted that, while this analysis primarily focuses on carbon storage benefits associated with the carbon content of the panel, additional exogenous $CO_2$ is sequestered by the carbon capture plant and stored in the ground. When considering these additional carbon storage benefits, as well as renewable energy and recycled HDPE, carbon neutrality may be achieved in as little as 20 years. We are currently exploring alternative approaches to more holistically look at the global warming benefits associated with the sequestration and storage of $CO_2$. It is noted that although the estimated minimum selling price of $CO_2$LIG filler of both lignin cases are higher than that of the lignite case and the market price of wood flour due to the higher feedstock cost, both lignin cases has much lower GWP. Assuming the same greenhouse gas emission in the downstream composite synthesis step and

using the GWP of a conventional woody composition as a baseline, an emission reduction of approximate 0.47 and 0.26 kg $CO_{2,eq}$ per kg composite can be achieved *via* the Lignin-HCl and Lignin-$H_2SO_4$ approach, respectively.[43] A carbon price of roughly $340 and $1600 per tonne $CO_2$ will be required to bring the estimated minimum selling price of the Lignin-HCl and Lignin-$H_2SO_4$ cases down from $0.83 and $1.29 per kg to $0.55 per kg, comparable to the market price of wood flour.

# Experimental

## Reagents

The lignite, Department of Energy Coal Sample-25 (DECS-25), was sourced from the Penn State Coal Bank (**https://www.energy.psu.edu/facilities/penn-state-coal-sample-bank**). The materials were ground and sieved with a 625 mesh. The lignite was dried at 80 °C for 24 hours. Alkaline lignin was sourced from TCI America. ACS reagent grade sulfuric acid was purchased from Sigma-Aldrich.

## Carboxylation reactions

### Reactions in parr autoclaves

*Alkaline lignin.* Alkaline lignin (500 g) was added to a 2 L Parr vessel equipped with a thermal couple. The Parr vessel was sealed, and $CO_2$ (400 psig) was introduced at room temperature. The reactor contents were heated to 80 °C under a nominal 1 °C $min^{-1}$ ramp rate and held at the same temperature for 1 h. The reactor was allowed to cool naturally to room temperature and then depressurized.

*Lignite.* Experimental details for the carboxylation of lignite were adopted from the aforementioned reaction sequence for lignin with slight modifications. Briefly, a Parr reactor was charged with 500 g of lignite and NaOH (16 g, 2 mL 1 M NaOH per g lignite). The Parr reactor was then heated to 130 °C and stayed for an hour, after which excess amount of steam was vented, and $CO_2$ (g) was charged to 400 psig (28 bar) at the same temperature. The Parr reactor was kept under the same conditions for an additional hour and then slowly cooled to room temperature and the pressure carefully released.

### Isolation and work-up

*Alkaline lignin.* Following the reaction, alkaline lignin was transferred to four separate 500 mL centrifugation cups (120 g per ea). Aqueous sulfuric acid (1 M, 0.12 L) was added to the centrifugation cup and mixed with water to form a slurry. The slurry was centrifuged, the supernatant removed, and water (0.15 L) added. This process was repeated until the pH of the supernatant was >4. The lignin paste was dried in a vacuum oven at 80 °C.

*Lignite.* The lignite was separately transferred to a wide-mouth plastic jar and acidified by aqueous sulfuric acid (2 mL 1 M solution per g lignite) with water (100 mL per g lignite). The black paste mixture was thoroughly mixed and washed with excess water over a medium-frit filter funnel under vacuum. The lignite was then dried in a vacuum oven at 60 °C.

## Carboxylation quantification

**Nuclear magnetic resonance (NMR).** The $^{13}C$ magic angle spinning NMR spectra were collected on a 600 MHz Bruker Avance III spectrometer using 5 mm zirconia rotors spinning at 3–5 kHz, a home-built custom HX probe and an in-house-developed WHiMS rotor system.

**FT-IR (Fourier transform infrared) spectroscopy.** Alkaline lignin was mixed with sodium hydroxide (1 M) at a ratio of 1 g lignin to 1 mL NaOH. Additional samples with increased millimoles of base at a ratio of 1 : 2 for alkaline lignin and 1 : 2, 1 : 3, and 1 : 4 for lignite were also reacted. The resulting slurry was dried on a hot plate. The dried sample was ground in a mortar and pestle until a fine power was produced. The alkaline lignin/NaOH powder was mixed with potassium bromide as a 1 : 1 ratio. Approximately 0.075 g of this mixture was loaded into the high temperature DRIFTs cell. The experimental procedure was performed *in situ* with each spectrum the result of 16 co-added scans and a spectral resolution of 4 $cm^{-1}$. The DRIFTs cell was purged with nitrogen to remove air and water vapor from the cell. The nitrogen gas was replaced with $CO_2$ and the cell was purged with $CO_2$. The cell was pressurized to a 250–260 psig. After two minutes, the heating profile was started at a rate of 5 °C $min^{-1}$ with a target set point of 130 °C. Isothermal conditions were maintained for thirty minutes before cooling the cell to room temperature followed by a nitrogen purge to remove $CO_2$ from the cell.

**Composite manufacturing.** HDPE and fillers were dry mixed using a ball mill in the predetermined material ratios. Following this, they were melt-compounded using a HAAKE Rheomix and then granulated in a Brabender mixer. Subsequently, the polymer composites were injection molded in flexural samples with dimensions per ASTM D790. Two stage processing was used to manufacture the polymer composites with unfunctionalized and functionalized fillers. Injection molding was used to manufacture lignin polymer composites with 50 wt% filler. Additionally, friction extrusion performed on a shear assisted processing and extrusion (ShAPE™) machine was used to manufacture the polymer composites with 80 wt% fillers. The granulated composites with 80 wt% functionalized and unfunctionalized fillers were loaded into the extrusion ring of the ShAPE™ machine and cold compacted in multiple stages to form the billet that was subjected to extrusion. During friction extrusion on the ShAPE™ equipment, a rotating die impinges onto the stationary billet. Due to the friction between the billet material and the extrusion die along with the mechanical forces imparted, the billet material heats up (in the absence of external heating), plasticizes and flows through a cavity in the die to form the extrudate.

**Composite property testing.** Flexure properties of composites were measured on the Instron 5582 servo-electric test frame with a 500 N load cell and a three-point bending fixture. Specimens were cut to 58.5 mm × 12.7 mm × 3 mm and the span (the distance between supports) was 50 mm. Flexural tests were performed following the procedure A in ASTM D790.

 

The nominal crosshead speed was set to 1.27 mm $min^{-1}$ targeting at obtaining the 1%/min nominal strain rate. Midspan deflection was recorded by an optical extensometer (Epsilon One) for modulus calculation.

**TEA and LCA.** TEA and LCA were conducted based on experimental data to evaluate the economic feasibility and environmental benefit of the $CO_2$LIG technology. The system boundaries of both TEA and LCA for the lignin and lignite cases are detailed in Fig. S1.† Rigorous process models were developed in Aspen Plus V12 for both carbon capture and carboxylation units to calculate the mass and energy balance and size key equipment. Mass and energy balance and life cycle inventory (LCI) of upstream and downstream units were collected from commercial LCI databases or open literature and summarized in Table S3.† The capital cost of equipment was estimated using Aspen Process Economic Analyzer V12. The key economic and pricing assumptions can be found in Table S2.†

In the Aspen Plus process model, EEMPA, a water-lean solvent developed by Pacific Northwest National Laboratory, was used to capture $CO_2$ from flue gas, which has an estimated carbon capture cost much lower than conventional aqueous amine technologies.[1] Due to the challenges in recovering $CO_2$ functionalized lignin or lignite ($CO_2$LIG filler) in solutions, two acid treatment approaches, one using HCl and the other using $H_2SO_4$, were investigated for the carboxylation unit, of which process flow diagrams were shown in Fig. S5.† In Aspen Plus V12, ELENRTL property package was selected for the carboxylation unit, while Aspen built-in Elec Wizard was used to generate electrolyte reactions of NaOH, $CO_2$, $H_2SO_4$, and HCl in the aqueous solution. Reactions involved in NaOH pretreatment, carboxylation, and acidification steps are summarized in Fig. S6,† where phenol was used to represent the active site in the lignin or lignite surface. Lignin, lignite, and their derivatives were simulated as conventional solids given CHONS, basic property data (heat of formation, heat capacity, and density) using the method developed by Wooley and Putsche (1996).[2] Operating conditions, carboxylation rate, and product recovery rate for all lignin and lignite cases were specified based on experimental data summarized in Table S2.†

The environmental impacts of the $CO_2$LIG-plastic composite panel were evaluated using an LCA approach. The LCA was performed based on the ISO 14 040 and 14 044 standards.[45,46] The functional unit of the study was 1 kg of $CO_2$LIG-plastic composite panel. The system boundary was cradle-to-gate and included all the input and output flows from the acquisition of the raw materials ("cradle") until $CO_2$LIG-plastic composite panel manufacturing ("gate"). The main processes included in the system boundary are represented in Fig. S4.† The analysis was performed using the software SimaPro v.9 and the environmental impacts were evaluated using the Tool for the Reduction and Assessment of Chemical and Other Environmental Impacts (TRACI) v.2.1.[47] The mass and energy balances from the chemical process simulation in AspenPlus were used for the LCI. The LCI databases DATASMART, USLCI, and Ecoinvent v.3.5 were used for the analysis.[40] A cut-off approach was considered to allocate the impacts between coproducts. Based on the cut-off approach the impacts associated with the plant releasing $CO_2$ were allocated to the primary product (*e.g.*, electricity) and $CO_2$ was considered a waste product available burden free from the plant. The impacts associated with the carbon capture plant were allocated to the $CO_2$ product.

The results were expressed in terms of GWP over a 100-year time horizon and reported in terms of $CO_2$ equivalent ($CO_{2e}$). The overall environmental impacts associated with the production of $CO_2$LIG-plastic composite were compared against the environmental impacts of corresponding conventional or petroleum-based composite materials.[43] Two main components were considered in the evaluation of the GWP: (i) the impact on global warming associated with fossil-based greenhouse gas emissions released throughout the life cycle of the $CO_2$LIG-plastic composite panel and (ii) the carbon storage benefits associated with storing carbon over the lifetime of the panel, which included the carbon stored in the lignin component of the panel, and the $CO_2$ sequestered and stored in the panel. It should be noted that, unlike the lignin case, the carbon stored in the lignite component of the panel was not accounted for because it is fossil-based. The carbon stored in the lignin component of the carbon is biogenic and the carbon sequestered in the forest is assumed to be equal to the carbon released at the end of life of the product. By keeping the carbon sequestered in the panel, there is an overall beneficial effect on global warming which is dependent on the numbers of years of storage (lifetime of the material). In the case of lignite, the carbon is fossil-based and will take millions of years to replenish. Therefore, we accounted for no net beneficial effect on global warming by keeping the lignite carbon stored in the panel.

## Conclusions

In summary, this work details how $CO_2$ can be chemically fixed on lignin or lignite surfaces as well as the economic viability of using lignin or lignite composite materials for $CO_2$ removal. The composites are equivalent to the standard WPCs for decking, fencing, and lawn furniture composed of wood flour embedded in an HDPE matrix, with the added benefit of $CO_2$ sequestration. These composite materials can become $CO_2$-negative by replacing wood flour filler with particles of lignin or lignite with surface-fixed $CO_2$.

The $CO_2$ is chemically added to lignin or lignite surface *via* the KS reaction, creating carboxylic acids at the lignin or lignite particle's surface *via* a durable C–C bond. The carboxylation ($CO_2$ fixation) is completed after acid workup followed by filtering and drying. Isolated yields were as high as 94% for lignin and 80% for lignite particles. Speciation and quantification of $CO_2$ loading was performed using high-pressure magic angle spinning NMR and DRIFTS with final $CO_2$ loadings of approximately 2.0–4.2 wt% for the lignite and lignin fillers, respectively.

Carboxylated and uncarboxylated lignin and lignite polymer composites were manufactured using conventional injection molding and friction extrusion using the ShAPE process. Injection molding accommodated only about ~50 wt% fillers, whereas friction extruded composites could be manufactured with filler concentrations of 80 wt%. Friction extruded composites with 80 wt% carboxylated lignin and lignite fillers showed the flexural strength and moduli required to meet the uniform live load bearing capacity required by IBC, allowing them to be qualified as decking materials.

A TEA suggests that $CO_2$-functionalized lignin and lignite filler provide favorable economic potential. Carboxylated lignin can be produced as cheaply as \$0.83 per kg, while carboxylated lignite particles could be produced for \$0.37 per kg —at cost parity with wood flour fillers. A cradle to grave LCA shows that $CO_2$-functionalized lignite/HDPE composites have the potential to reduce greenhouse gas emissions over conventional WPC by up to 62%, while the $CO_2$-functionalized lignin composites can be $CO_2$-negative under various scenarios. When renewable electricity and recycled HDPE were considered, it would take 54 years to achieve net negative GWP. If the system boundary is expanded where additional captured $CO_2$ is sequestered in the ground, carbon neutrality could be achieved after 20 years of carbon storage.

## Author contributions

K. S. K. designed and oversaw the composite fabrication and testing; J. L. sourced precursors and supervised the carboxylation experiments and particle isolation; which were performed by W. J., N. N., J. K. designed conducted the IR experiments; Y. N., J. R., R. J., M. R. R., A. N., and E.N. fabricated the composites and tested their performance; Y. J. and F. P. designed and conducted the TEA and LCA modeling and analysis; D. J. H. and S. N. conceived and supervised the study. All authors wrote the paper.

## Data availability

The data supporting this article have been included as part of the ESI.†

## Conflicts of interest

There are no conflicts to declare.

## Acknowledgements

The authors are grateful to the United States Department of Energy (DOE) office of Fossil Energy and Carbon Management (FECM) under FWP 78606 and the Research, Development and Demonstration (RD&D) Program at SoCalGas for funding. The authors also thank Greg Coffey for grinding and sieving lignite samples and Eric Walter and Katarzyna Grubel for assisting with $^{13}C$ solid-state Nuclear Magnetic Resonance spectroscopy.

## References

1 H. L. J. Romero, *Climate Change 2023: Synthesis Report. Contribution of Working Groups I, II and III to the Sixth Assessment Report of the Intergovernmental Panel on Climate Change*, Geneva, Switzerland, 2023.
2 D. Baskaran, P. Saravanan, L. Nagarajan and H.-S. Byun, An overview of technologies for capturing, storing, and utilizing carbon dioxide: Technology readiness, large-scale demonstration, and cost, *Chem. Eng. J.*, 2024, **491**, 151998.
3 D. Y. Shu, S. Deutz, B. A. Winter, N. Baumgärtner, L. Leenders and A. Bardow, The role of carbon capture and storage to achieve net-zero energy systems: Trade-offs between economics and the environment, *Renewable Sustainable Energy Rev.*, 2023, **178**, 113246.
4 J. R. Diez, S. Tomé-Torquemada, A. Vicente, J. Reyes and G. A. Orcajo, Decarbonization Pathways, Strategies, and Use Cases to Achieve Net-Zero $CO_2$ Emissions in the Steelmaking Industry, *Energies*, 2023, **16**(21), 7360.
5 M. Ouikhalfan, O. Lakbita, A. Delhali, A. H. Assen and Y. Belmabkhout, Toward Net-Zero Emission Fertilizers Industry: Greenhouse GasEmission Analyses and Decarbonization Solutions, *Energy Fuel*, 2022, **36**(8), 4198–4223.
6 H. C. Lau and S. C. Tsai, Global Decarbonization: Current Status and What It Will Take to Achieve Net Zero by 2050, *Energies*, 2023, **16**(23), 7800.
7 **https://www.iea.org/commentaries/is-carbon-capture-too-expensive**.
8 **https://www.iea.org/reports/ccus-in-clean-energy-transitions**.
9 D. W. Keith, G. Holmes, D. St. Angelo and K. Heidel, A Process for Capturing $CO_2$ from the Atmosphere, *Joule*, 2018, **2**(8), 1573–1594.
10 M. A. Celia, Geological storage of captured carbon dioxide as a large-scale carbon mitigation option, *Water Resour. Res.*, 2017, **53**(5), 3527–3533.
11 D. J. Heldebrant, J. Kothandaraman, N. Mac Dowell and L. Brickett, Next steps for solvent-based $CO_2$ capture; integration of capture, conversion, and mineralisation, *Chem. Sci.*, 2022, **13**(22), 6445–6456.
12 J. Kothandaraman and D. J. Heldebrant, Towards environmentally benign capture and conversion: heterogeneous metal catalyzed $CO_2$ hydrogenation in $CO_2$ capture solvents, *Green Chem.*, 2020, **22**(3), 828–834.
13 J. Leclaire and D. J. Heldebrant, A call to (green) arms: a rallying cry for green chemistry and engineering for $CO_2$ capture, utilisation and storage, *Green Chem.*, 2018, **20**(22), 5058–5081.
14 C. Maeda, Y. Miyazaki and T. Ema, Recent progress in catalytic conversions of carbon dioxide, *Catal. Sci. Technol.*, 2014, **4**(6), 1482–1497.

 

15 Z. Huang, R. G. Grim, J. A. Schaidle and L. Tao, The economic outlook for converting $CO_2$ and electrons to molecules, *Energy Environ. Sci.*, 2021, **14**(7), 3664–3678.
16 B. Dziejarski, R. Krzyzynska and K. Andersson, Current status of carbon capture, utilization, and storage technologies in the global economy: A survey of technical assessment, *Fuel*, 2023, **342**, 127776.
17 A. Rafiee, K. R. Khalilpour, D. Milani and M. Panahi, Trends in $CO_2$ conversion and utilization: A review from process systems perspective, *J. Environ. Chem. Eng.*, 2018, **6**(5), 5771–5794.
18 O. Rueda, J. M. Mogollón, A. Tukker and L. Scherer, Negative-emissions technology portfolios to meet the 1.5 °C target, *Global Environ. Change*, 2021, **67**, 102238.
19 L. Desport and S. Selosse, Perspectives of $CO_2$ utilization as a negative emission technology, *Sustainable Energy Technol.*, 2022, **53**, 102623.
20 B. Shanks, C. Howe, S. Draper, H. Wong and C. Cheeseman, Carbon capture and storage in low-carbon concrete using products derived from olivine, *R. Soc. Open Sci.*, 2024, **11**(5), 231645.
21 CarbonBuilt Ultra-Low Carbon Concrete for Green Construction. Available from: **https://carbonbuilt.com/**.
22 CarbiCrete: Decarbonized Concrete. Available from: **https://carbicrete.com/**.
23 A. Rafighi, A. Dorostkar and M. Madhoushi, Investigation on mechanical properties of composite made of sawdust and high density Polyethylene, *Int. J Lignocellul. Prod.*, 2014, **1**(2), 134–141.
24 A. Najafi and S. K. Najafi, Effect of Load Levels and Plastic Type on Creep Behavior of Wood Sawdust/HDPE Composites, *J. Reinf. Plast. Compos.*, 2009, **28**(21), 2645–2653.
25 D. Bootkul, T. Butkul and S. Intarasiri, Physical and Mechanical Properties of Wood Plastic Composites from Teak Wood Sawdust and High Density Polyethylene (HDPE), *Key Eng. Mater.*, 2017, **751**, 277–282.
26 K. Komisarz, T. M. Majka and K. Pielichowski, Chemical and Physical Modification of Lignin for Green Polymeric Composite Materials, *Materials*, 2023, **16**(1), 16.
27 Y. Kosugi and K. Takahashi, Carboxylation reaction with carbon dioxide. Mechanistic studies on the Kolbe–Schmitt reaction, *Stud. Surf. Sci. Catal.*, 1998, **114**, 487–490.
28 A. S. Lindsey and H. Jeskey, The Kolbe–Schmitt Reaction, *Chem. Rev.*, 1957, **57**(4), 583–620.
29 N. Morinaga, M. Uchigashima, M. A. Rahim, K. Onishi, K. Takahashi and Y. Kosugi, The Kolbe–Schmitt reaction in aqueous solutions, *Nippon Kagaku Kaishi*, 2002, (3), 467–469.
30 J. T. Sun, C. Wang, L. P. Stubbs and C. B. He, Carboxylated Lignin as an Effective Cohardener for Enhancing Strength and Toughness of Epoxy, *Macromol. Mater. Eng.*, 2017, **302**(12), 1700341.
31 Y. J. Zhang, H. Wang, T. L. Eberhardt, Q. Gu and H. Pan, Preparation of carboxylated lignin-based epoxy resin with excellent mechanical properties, *Eur. Polym. J.*, 2021, **150**, 110389.
32 Y. Zhang, J. M. Li, X. X. Wu, D. Y. Wang, S. N. Zhou, S. B. Han, *et al.*, Simultaneously reinforcing and toughening of shape-memory epoxy resin with carboxylated lignosulfonate: Facile preparation and effect mechanism, *Int. J. Biol. Macromol.*, 2022, **217**, 243–254.
33 B. S. Taysom, N. Overman, M. Olszta, M. Reza-E-Rabby, T. Skszek, M. DiCiano and S. Whalen, Shear assisted processing and extrusion of enhanced strength aluminum, *Int. J. Mach. Tools Manuf.*, 2021, **169**, 103798.
34 G. A. Adam, *InventorLignin-based concrete admixtures*, 2013.
35 A. Chamas, L. Qi, H. S. Mehta, J. A. Sears, S. L. Scott, E. D. Walter and D. W. Hoyt, High temperature/pressure MAS-NMR for the study of dynamic processes in mixed phase systems, *Magn. Reson. Imaging*, 2019, **56**, 37–44.
36 E. D. Walter, L. Qi, A. Chamas, H. S. Mehta, J. A. Sears, S. L. Scott and D. W. Hoyt, MAS NMR Reaction Studies at High Temperatures and Pressures, *J. Phys. Chem. C*, 2018, **122**(15), 8209–8215.
37 S. Ok, S. Gautam, K. H. Liu and D. R. Cole, Surface Interactions and Nanoconfinement of Methane and Methane plus $CO_2$ Revealed by High-Pressure Magic Angle Spinning NMR Spectroscopy and Molecular Dynamics, *Membranes*, 2022, **12**(12), 1273.
38 F. H. Blindheim and J. Ruwoldt, The Effect of Sample Preparation Techniques on Lignin Fourier Transform Infrared Spectroscopy, *Polymers*, 2023, **15**(13), 2901.
39 ICC general codes: table 1607. 1 minimum uniformly distributed live loads, l0, and minimum concentrated live loads.
40 R. Frischknecht, N. Jungbluth, H. J. Althaus, G. Doka, R. Dones, T. Heck, *et al.*, The ecoinvent database: Overview and methodological framework, *Int. J. Life Cycle Assess.*, 2005, **10**(1), 3–9.
41 C. Culbertson, T. Treasure, R. Venditti, H. Jameel and R. Gonzalez, Life Cycle Assessment of lignin extraction in a softwood kraft pulp mill, *Nord. Pulp Pap. Res. J.*, 2016, **31**(1), 30–40.
42 Containers and Packaging: Product-Specific Data. **https://wwwepagov/facts-and-figures-about-materials-waste-and-recycling/containers-and-packaging-product-specific**.
43 P. F. Sommerhuber, J. L. Wenker, S. Rüter and A. Krause, Life cycle assessment of wood-plastic composites: Analysing alternative materials and identifying an environmental sound end-of-life option, *Resour., Conserv. Recycl.*, 2017, **117**, 235–248.
44 I. Ganguly, F. Pierobon and E. S. Hall, Global Warming Mitigating Role of Wood Products from Washington State's Private Forests, *Forests*, 2020, **11**(2), 194.
45 ISO aI. *Environmental management, Life cycle assessment, Principles and framework*, International Organization for Standardization, Geneva, 2006.
46 ISO bI. *Environmental management, Life cycle assessment. Requirements and guidelines*, International Organization for Standardization, Geneva, 2006.
47 J. Bare, *Tool for the Reduction and Assessment of Chemical and other Environmental Impacts (TRACI). Software Name and Version Number: TRACI version 2.1. User's Manual*. U.S. EPA., Washington, D.C.; 2012.